IDENTIFICATION OF NEUTRON ABSORBING ELEMENTS ON MERCURY'S SURFACE USING MESSENGER NEUTRON DATA. David J. Lawrence[1], William C. Feldman[2], John O. Goldsten[1], Sean C. Solomon[3], and the MESSENGER Science Team, [1]Johns Hopkins University Applied Physics Laboratory, 11100 Johns Hopkins Drive, Laurel, MD 20723 (David.J.Lawrence@jhuapl.edu), [2]Planetary Science Institute, Tucson, AZ 85719, [3]Carnegie Institution of Washington, Washington, DC 20005.

Introduction: Of all elements, Fe is key for understanding several aspects of Mercury's formation history [1], but currently there is little definitive information about Mercury's surface Fe abundance. In addition, there is large uncertainty about the elemental source of Mercury's low albedo [2], which in principle could be caused by enhanced concentrations of Fe, Ti and/or C. Thermal neutrons on Mercury's surface, resulting from the moderation of fast neutrons induced by galactic cosmic rays (GCRs) and measured by the MESSENGER Neutron Spectrometer (NS), are highly sensitive to the presence of Fe and Ti [3,4], as well as the presence of the rare-earth elements Gd and Sm [5]. The identification of these elements from thermal neutrons is not unique, but when thermal neutron data are combined with other composition data (e.g., gamma-ray), unique measures of various elemental abundances can be obtained [e.g., 3]. Here we present data from the first two MESSENGER flybys of Mercury and an analysis of data from the first flyby where thermal neutrons from Mercury were measured using spacecraft Doppler filter effects. The data and analysis presented here enable us to provide preliminary estimates of the neutron absorptive nature of Mercury's surface.

Mercury Flyby Data: The MESSENGER NS contains three separate neutron sensors [6], two of which (Lithium Glass 1 and 2 or LG1 and LG2) are sensitive to thermal neutrons. The LG sensors are planar scintillator detectors that are oriented with their normal vectors either parallel (LG1) or anti-parallel (LG2) to the spacecraft x-axis (see Fig. 1). Using principles of neutron Doppler filter spectroscopy [7], an enhancement of thermal neutrons is measured when the spacecraft velocity vector is in line with the sensor normal vector; a relative decrease in thermal neutrons occurs when the spacecraft velocity vector is anti-parallel to the sensor normal; finally, no Doppler effect occurs when the spacecraft velocity vector is perpendicular to the sensor normal vector. Figure 2 shows LG counting rate data from MESSENGER's two Mercury flybys (M1 and M2) along with spacecraft orientation data with respect to the spacecraft velocity vector (expressed as $(\mathbf{V}\bullet\hat{x})/|\mathbf{V}|$, where $\mathbf{V}$ is the spacecraft velocity vector and $\hat{x}$ is the x-axis unit vector). During both flybys, the spacecraft executed various orientation maneuvers that changed its orientation with respect to the spacecraft velocity vector. Specifically, at the times 18:50 and 18:59 UTC for M1 and 8:31 for M2, the spacecraft rotated such that LG2 measured enhanced thermal neutrons. These enhancements correspond to times when $(\mathbf{V}\bullet\hat{x})/|\mathbf{V}|$ was close to -1. Since these thermal neutron enhancement signatures are significantly above the background counting rate and their statistical precision, they may provide a sensitive measure of thermal neutrons and hence the abundance of neutron-absorbing elements.

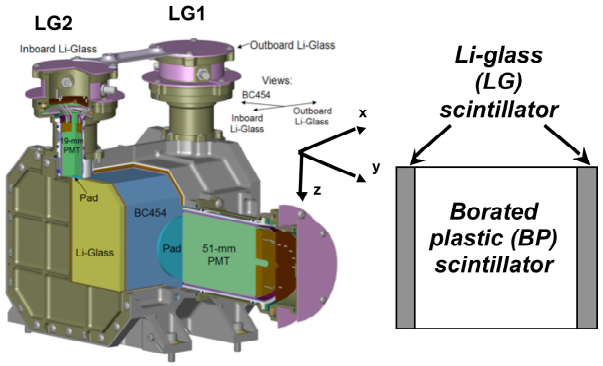

Figure 1. MESSENGER NS showing three sensors and orientation with respect to the spacecraft coordinate system.

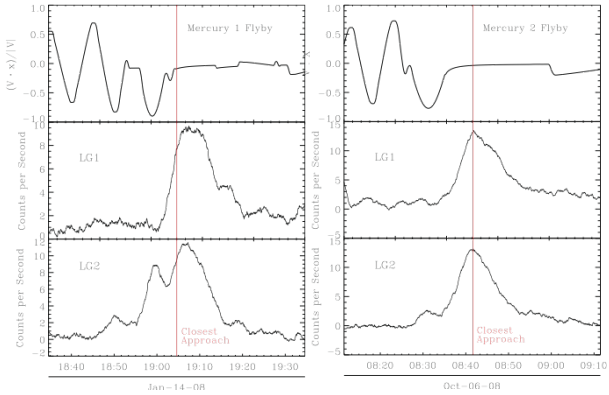

Figure 2. LG1 and LG2 data from M1 (left) and M2 (right). The top panels show the spacecraft orientation with respect to the spacecraft velocity. The bottom panels show the LG1 and LG2 data after being smoothed with an 80-s moving window.

Neutron Count Rate Model: In order to properly understand the measured neutron data, effects on the data from the spacecraft and Mercury's surface need to be modeled. Feldman et al. [8] give a generalized expression of the measured neutron counting rate, C, from a moving spacecraft around a planet:

$$C = \frac{1}{2\pi}\int d\phi \int d\mu \int dK \left[\frac{\mathbf{V}\bullet\hat{n}}{V}\right] A_\varepsilon(K,\theta,\phi)\Phi(K,\theta) \quad (1)$$

The integral is carried out over energy K and instrument-centered angles θ (or μ=cos(θ)) and ϕ. The GCR-induced neutron flux, Φ (assumed here to be

azimuthally symmetric and integrated over ϕ) is modeled for a variety of soil compositions at room temperature using the particle transport code MCNPX. Effects due to Mercury's gravity and 3D spherical geometry are explicitly included. The area-efficiency response of the NS, A_ε, includes effects due to both the sensor efficiency and spacecraft materials. A_ε was modeled using MCNPX; the spacecraft and NS were characterized with 100+ geometry elements. We obtained a preliminary verification of the code by reproducing the absolute count rate of Lunar Prospector neutron data [9] to within 15–20%.

Preliminary Results: Figure 3 shows the modeling results of LG1 and LG2 for the M1 flyby overplotted on the same smoothed data shown in Fig. 1. The only free parameter applied to the model was a multiplicative normalization constant of 2.99. Modeling results for M2 will be considered in a later study. To calculate the model, we used three non-hydrated lunar soil compositions we expect to be analogous to the unknown Mercury composition. In order to span a large range of neutron absorption, we used soils ranging from low neutron absorption (ferroan anorthosite, FAN) to moderate neutron absorption (Luna 20), to high neutron absorption (Apollo 11). The results show that for the LG1 data, there is little differentiation for the three different soil types. Since LG1 was not highly sensitive to thermal neutrons for the M1 spacecraft orientations, this result is expected. In contrast, the thermal neutron enhancement peak at 18:59 is highly sensitive to the neutron absorption content of the soil. In preliminary models, we also varied the surface temperature of the FAN fluxes from 100 to 400 K and found that different temperatures could cause variations (not shown) in the relative height of the 18:59 peak by up to 25%, with lower temperatures giving lower peak heights. Since the measurement at 18:59 was made just prior to dawn on the Mercury surface (with a consequent surface temperature as low as 100 K [10]), the models shown may be overestimated by up to 25%.

In summary, these results indicate that the measured data are most consistent with a neutron absorption that is between Luna 20 and Apollo 11 type soils, which have a wide range of Fe (5.8-12.8 wt.%), Ti (0.3-4.8 wt.%), Gd (4.4-18 ppm), and Sm (3.2-14 ppm) contents [9]. Our improved model suggests higher abundances of neutron-absorbing elements than our initial estimate [11] that the neutron absorption was less than a total Fe equivalent of 6 wt.%. The main reason for this revised estimate is that we are now fully accounting for how the spacecraft material affects the neutron data as well as starting to understand surface temperature effects. These model results are preliminary and the sensitivity of the model to effects such as spacecraft mass distribution, spacecraft fuel loading, and surface temperature will need to be investigated prior to concluding that Mercury's surface has higher abundances of neutron absorbing elements than previously suggested.

References: [1] Strom R.G. and A.L. Sprague (2003) *Exploring Mercury*, Springer. [2] Denevi B.W. and M.S. Robinson (2008) *Icarus*, 197, 239. [3] Feldman W.C. et al. (2000) *JGR*, 105, 20347. [4] Elphic R.C. et al. (2002) *JGR*, 107, 10.1029/2000JE001460. [5] Elphic R.C. et al. (2000) *JGR*, 105, 20333. [6] Goldsten J.O. et al. (2007) *Space Sci. Rev.*, 131, 339. [7] Feldman W.C. et al. (1986) *Nuc. Inst. and Methods*, A245, 182. [8] Feldman W.C. et al. (1989) *JGR*, 94, 513. [9] Lawrence D.J. et al. (2006) *JGR*, 111, 10.1029/2005JE002637. [10] Lodders K. and B. Fegley, Jr. (1998) *The Planetary Scientist's Companion*. [11] Solomon S.C. et al. (2008) *Science*, 321, 59.

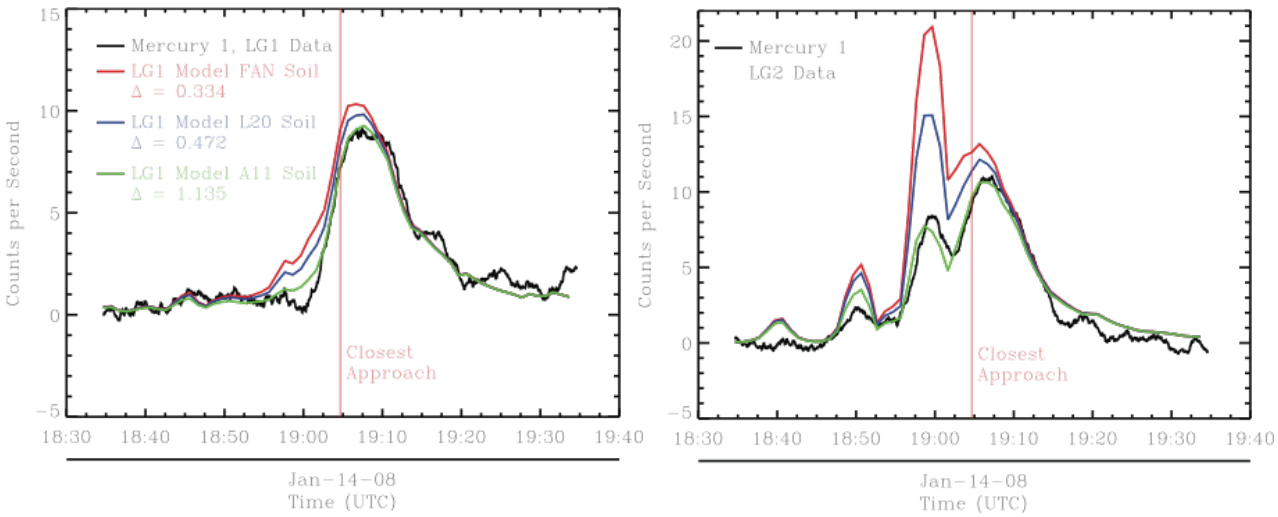

Figure 3. Model results for LG1 (left) and LG2 (right) using three different lunar-type soils of FAN (red), Luna 20 (blue), and Apollo 11 (green). Smoothed LG1 and LG2 are shown in black.